



Physicochemical study and corrosion inhibition potential of dithiolo[4,5-b][1,4]dithiepine for mild steel in acidic medium

D. Jeroundi¹, H. Elmsellem^{2*}, S. Chakroune¹, R. Idouhli³, A. Elyoussfi², A. Dafali², E. M. El Hadrami¹, A. Ben-Tama¹, Y. Kandri Rodi¹

¹ Laboratoire de Chimie Organique Appliquée, Université Sidi Mohamed Ben Abdellah, Faculté des Sciences et Techniques, Route d'Immouzer, BP 2202, Fès, Morocco.

² Laboratoire de chimie analytique appliquée, matériaux et environnement (LC2AME), Faculté des Sciences, B.P. 717, 60000 Oujda, Morocco

³ Laboratory of Physical Chemistry of Materials and Environment, Department of Chemistry, University Cadi Ayyad, Faculty of Science Semlalia, BP 2390 Marrakech, Morocco.

Received 14 June 2016, Revised 27 Aug 2016, Accepted 1 Sept 2016

*Corresponding author. E-mail: h.elmsellem@yahoo.fr Tél: +212670923431

Abstract

The effect of dithiolo[4,5-b][1,4]dithiepine(P1) dye on the electrochemical corrosion of mild steel in HCl solutions was studied using gravimetric techniques at 308K. The results indicate that dithiolo[4,5-b][1,4]dithiepine(P1) acts as an inhibitor in the acidic corrodent. The inhibition efficiency was observed to be sensitive to acid concentration and increased with an increase in (P1) concentration. The experimental data were corroborated with the Langmuir as well adsorption isotherms. The activation energy values of 40.70 kJ mol⁻¹ calculated for the corrosion process in the absence and presence of (P1) suggest that the inhibitor molecules are chemisorption adsorbed on the mild steel surface.

Keywords: Mild steel, dithiolo[4,5-b][1,4]dithiepine, Inhibition efficiency, DFT, Fukui function, Adsorption isotherm.

1. Introduction

Nowadays most important considerations in industry are reduction of overall costs by protection and maintenance of materials used. The protection of corroding metal surface prevents the waste of resources and money during the industrial applications and is vital to extend the equipment's lifetime; limiting the dissolution into the environment of toxic metals from the components [1-2].

Mild steel is extensively used in different industries in the merit of its good structural properties, good mechanical workability and low cost. Corrosion can be minimized using suitable preventive measures, and several techniques have been developed [3] to control corrosion. Corrosion inhibition of mild steel in acid solutions has become one of the most urgent and severe challenges in acid pickling process [4]. Mild steel is exposed to the action of acid in industrial processes in which acids have important functions, for example in oil well acidification, acid pickling, acid cleaning, and acid descaling. Use of inhibitors is one of the best methods of protecting metals against corrosion [5]. Corrosion inhibitors are compounds that are added in small quantities to an environment to prevent corrosion of metals [6-7]. Most of the efficient acid inhibitors are organic compounds containing nitrogen, sulphur and/or oxygen atoms in their molecule [8-10].

The purpose of the study is to investigate the inhibiting influence of dithiolo[4,5-b][1,4]dithiepine(P1) as a green inhibitor on mild steel corrosion in 1 M HCl acid solution. Gravimetric, electrochemical and DFT techniques was used in the study.

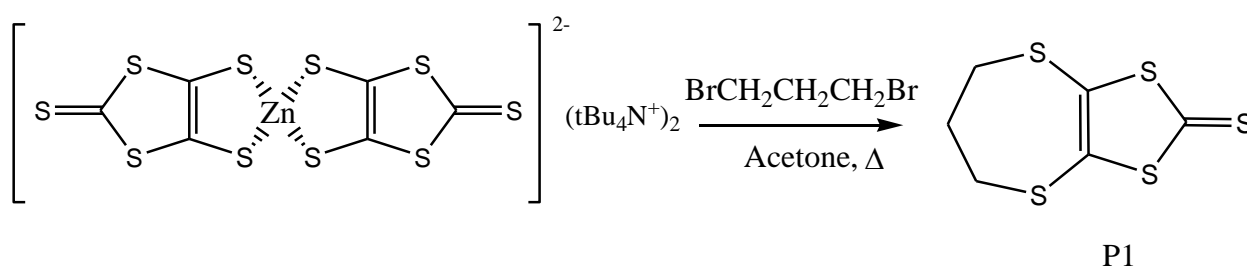
2. Experimental

2.1. Materials and solutions

The mild steel strips having a composition (wt.%) of 0.09% P, 0.01 % Al, 0.38 % Si, 0.05 % Mn, 0.21 % C, The mild steel used in the studies was analyzed using optical emission spectrometry and consists (in % weight): C = 0.253; Si = 0.12; P = 0.013; S = 0.024; Cr = 0.012; Mn = 0.03; and 99.548 Fe. The metal sheet was cut into coupon with the following dimensions of 1.5 x 1.5 x 0.05 cm³ and used for corrosion studies.

2.2. Synthesis of inhibitor

To a solution of zinc complex (5, 3mmol) in 80 ml of acetone was added 1, 3- dibromopropane (11, 6mmol) and refluxed under nitrogen for 6h. The solution turns orange, cooled to 0°C and the precipitate formed is filtered, washed with cold acetone to give T1 as a yellow powder. (Schema 1):



Scheme 1: Synthesis of dithiolo[4,5-b][1,4]dithiepine(**P1**).

The analytical and spectroscopic data are conforming to the structure of compound formed:

(P1): Yield: 69%; **mp:** 515 K; **RMN¹H (DMSO-d₆) δ ppm:** 2,48(2H,m,CH₂) ; 2,76(4H,m,SCH₂); **RMN¹³C (DMSO-d₆) δ ppm:** 33,21(2C, SCH₂); 34,08(CH₂); 140,01(2C,C=C); 211,44(C=S).

2.3. Gravimetric technique

Gravimetric experiments were performed according to the standard methods [11], the carbon steel specimens (1.5 cm × 1.5 cm × 0.05 cm) were abraded with a series of emery papers SiC (120, 600, and 1200 grades) and then washed with distilled water and acetone. After weighing accurately, the specimens were immersed in a 100 mL of 1.0 M HCl solution with and without addition of different concentrations of inhibitor P1.

All the aggressive acid solutions were open to air. After 6 hours of acid immersion, the specimens were taken out, washed, dried, and weighed accurately. In order to get good reproducibility, all measurements were performed few times and average values were reported.

2.4. Electrochemical measurements

The electrochemical measurements were carried out using Volta lab (Tacussel - Radiometer PGZ 100) potentiostat controlled by Tacussel corrosion analysis software model (Voltmaster 4) at static condition. The corrosion cell used had three electrodes. The reference electrode was a saturated calomel electrode (SCE). A platinum electrode was used as auxiliary electrode of surface area of 1 cm². The working electrode was carbon steel of the surface 1cm². All potentials given in this study were referred to this reference electrode. The working electrode was immersed in the test solution for 30 minutes to establish a steady state open circuit potential (E_{ocp}). After measuring the E_{ocp}, the electrochemical measurements were performed. All electrochemical tests have been performed in aerated solutions at 308 K.

The percentage of inhibition efficiency E_p was calculated following this equation [12]:

$$E_p\% = \frac{i_{cor(0)} - i_{cor(inh)}}{i_{cor(0)}} \times 100 \quad (1)$$

Where *i*_{corr}(0) and *i*_{corr}(inh) represent corrosion current density values without and with the inhibitor, respectively.

The EIS experiments were conducted in the frequency range with high limit of 100 kHz and different low limit 0.1 Hz at open circuit potential, with 10 points per decade, at the rest potential, after 30 min of acid immersion, by applying 10 mV ac voltage peak-to-peak. Nyquist plots were made from these experiments. The best semicircle can be fit through the data points in the Nyquist plot using a non-linear least square fit so as to give the intersections with the x-axis.

The inhibition efficiency of the inhibitor was calculated from the charge transfer resistance values using the following equation:

$$E\% = \frac{R_{ct}^{\circ} - R_{ct}}{R_{ct}} \times 100 \quad (2)$$

Where, R_{ct}° and R_{ct} are the charge transfer resistance in absence and in presence of inhibitor, respectively.

2.5. Quantum chemical calculations

Quantum chemical calculations are used to correlate experimental data for inhibitors obtained from different techniques (viz., electrochemical and weight loss) and their structural and electronic properties. According to Koopman's theorem [13], E_{HOMO} and E_{LUMO} of the inhibitor molecule are related to the ionization potential (I) and the electron affinity (A), respectively. The ionization potential and the electron affinity are defined as $I = -E_{HOMO}$ and $A = -E_{LUMO}$, respectively. Then absolute electronegativity (χ) and global hardness (η) of the inhibitor molecule are approximated as follows [14]:

$$\chi = \frac{I+A}{2}, \quad \chi = -\frac{1}{2}(E_{HOMO} + E_{LUMO}) \quad (3)$$

$$\eta = \frac{I-A}{2}, \quad \eta = -\frac{1}{2}(E_{HOMO} - E_{LUMO}) \quad (4)$$

Where $I = -E_{HOMO}$ and $A = -E_{LUMO}$ are the ionization potential and electron affinity respectively.

The fraction of transferred electrons ΔN was calculated according to Pearson theory [15]. This parameter evaluates the electronic flow in a reaction of two systems with different electronegativities, in particular case; a metallic surface (Fe) and an inhibitor molecule. ΔN is given as follows:

$$\Delta N = \frac{\chi_{Fe} - \chi_{inh}}{2(\eta_{Fe} + \eta_{inh})} \quad (5)$$

Where χ_{Fe} and χ_{inh} denote the absolute electronegativity of an iron atom (Fe) and the inhibitor molecule, respectively; η_{Fe} and η_{inh} denote the absolute hardness of Fe atom and the inhibitor molecule, respectively. In order to apply the eq. 5 in the present study, a theoretical value for the electronegativity of bulk iron was used $\chi_{Fe} = 7$ eV and a global hardness of $\eta_{Fe} = 0$, by assuming that for a metallic bulk $I = A$ because they are softer than the neutral metallic atoms [15].

The electrophilicity has been introduced by Sastri et al. [16], is a descriptor of reactivity that allows a quantitative classification of the global electrophilic nature of a compound within a relative scale. They have proposed the ω as a measure of energy lowering owing to maximal electron flow between donor and acceptor and ω is defined as follows.

$$\omega = \frac{\chi^2}{2\eta} \quad (6)$$

The Softness σ is defined as the inverse of the η [17]

$$\sigma = \frac{1}{\eta} \quad (7)$$

Using left and right derivatives with respect to the number of electrons, electrophilic and nucleophilic Fukui functions for a site k in a molecule can be defined [18].

$$f_k^+ = P_k(N+1) - P_k(N) \quad \text{for nucleophilic attack} \quad (8)$$

$$f_k^- = P_k(N) - P_k(N-1) \quad \text{for electrophilic attack} \quad (9)$$

$$f_k^{\cdot} = [P_k(N+1) - P_k(N-1)]/2 \quad \text{for radical attack} \quad (10)$$

where, $P_k(N)$, $P_k(N+1)$ and $P_k(N-1)$ are the natural populations for the atom k in the neutral, anionic and cationic species respectively.

3. Results and discussion

3.1. Weight loss measurements

The mass losses of mild steel coupon in 1 M HCl solution, with or without different concentrations of the investigated inhibitor, were recorded after 6h of immersion at temperature 308K. The corrosion rate of mild steel was calculated using the Equation 11.

$$v_{\text{corr}} = \Delta m / S.t \quad (11)$$

Where Δm is the mass lost (in grams), S is the surface area of the coupon (in cm^2) and t is the period of exposure (in hours)

Figure 1 shows the variation in mass loss for mild steel in the absence and presence of inhibitor. It is evident that the mass loss of mild steel for blank solution is much higher than that obtained for solution containing various concentrations of *PI*. Mass loss decreases with increase concentration of inhibitor. This implies that the presence of the inhibitor showed significant impact on the corrosion rate of mild steel in 1M HCl.

The inhibition efficiency and surface coverage were calculated from the mass loss data according to the Equations 12 and 13, respectively. Figure 2 shows the inhibition efficiency in different concentration of the leaf extract and it could be seen that the %E increases linearly with the inhibitor concentration.

$$E_w \% = \frac{V_{\text{blank}} - V_{\text{inh}}}{V_{\text{blank}}} \times 100 \quad (12)$$

$$\Theta = E_w / 100 \quad (13)$$

Where V_{inh} and V_{blank} are the corrosion rates in the absence and presence of inhibitor, respectively. It can be observed that the inhibition efficiency increased and the corrosion rate decreased as the inhibitor concentration increased. The maximum value of inhibition efficiency was 90%. It could be considered that dithiolo[4,5-b][1,4]dithiepine(*P1*). As inhibitor of mild steel to 1M HCl solution given the high level of the inhibition efficiency.

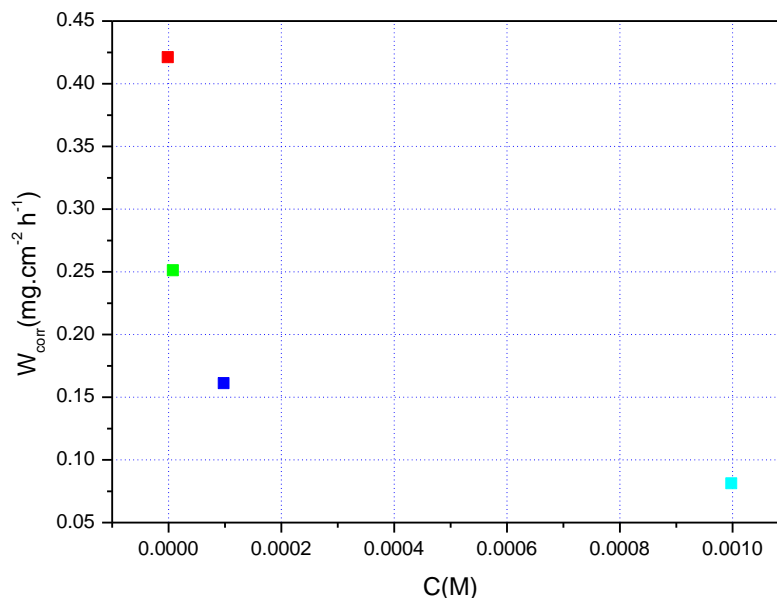


Figure 1: corrosion rate for mild steel in the different concentration of *PI* at 308K exposure for 6h.

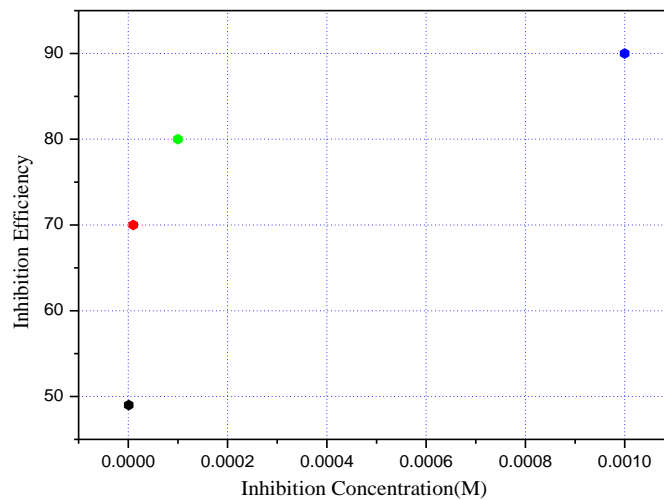


Figure 2: Inhibition efficiency of *PI* for mild steel in 1M HCl solution.

3.2. Adsorption Isotherm

The inhibition process in an acid environment occurs by appropriate adsorption of inhibitor molecules under study at the interface metal / solution and the adsorption process occurs as a result of the existence of electrostatic attraction between:

1. Metal-charged and the particles of charged inhibitor.
2. The polar interaction between uncharged inhibitor molecules with the metal.
3. Interaction of the type π with the metal.
4. All of the above.

The adsorption process depends on the electronic structure of the inhibitor, the nature of metal surface, reaction temperature and the number of active centers on the surface [19].

The most probably mechanism by which organic compounds inhibit metal corrosion is the adsorption organic molecules on the metallic surface.

Adsorption isotherms can provide significant information about the nature of interactions that exist at the metal/solution interface where both the water and inhibitor molecules are present.

In the present study, several adsorption isotherms were tested in an attempt to fit the experimental data but only the Langmuir adsorption isotherm provided acceptable linear fits based on the near unity values of the correlation coefficient (R^2) values. The linear form of the Langmuir adsorption isotherm can be expressed as [20]:

$$\frac{\theta}{1-\theta} = K_{ads} C_{inh} \quad (14)$$

By rearranging this equation :

$$\frac{C_{inh}}{\theta} = \frac{1}{K_{ads}} + C_{inh} \quad (15)$$

Where K_{ads} is the adsorption equilibrium constant, C_{inh} is the inhibitor concentration, and θ is the surface coverage.

The standard free energy of adsorption (ΔG_{ads}°) can be determined by the following equation:

$$\Delta G_{ads}^\circ = -RT \ln(55.5 K_{ads}) \quad (16)$$

Where R is the gas constant ($8.314 \text{ J K}^{-1} \text{ mol}^{-1}$), T is the absolute temperature (K), the value 55.5 is the concentration of water in solution expressed in M [21].

The values of K_{ads} and ΔG_{ads}° for the studied compound are reported in Table 1. The significantly large values of K_{ads} obtained for the studied inhibitor suggest strong adsorption of the molecules on mild steel surface. The use of ΔG_{ads}° value to describe the mode of adsorption of inhibitor molecules on metallic surface has been widely discussed [22- 24].

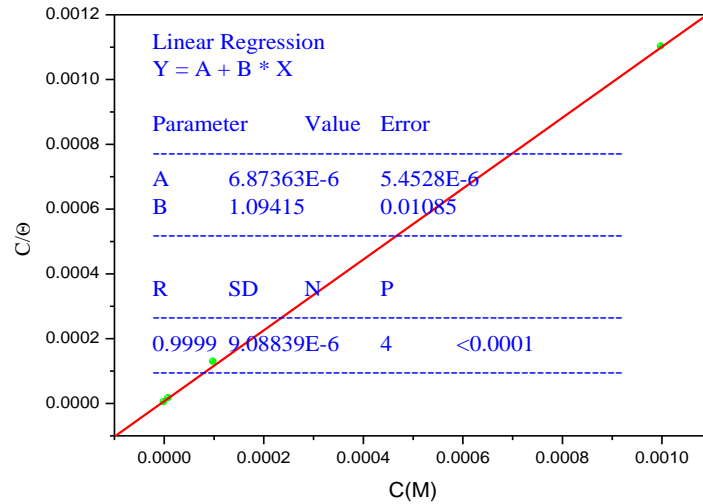


Figure 3: shows the plots of C_{inh}/θ versus C_{inh} and the estimated linear correlation is obtained for P1.

Table 1: Thermodynamic parameters for the adsorption of P1 in 1.0 M HCl on the mild steel at 308 K.

Inhibitor	$K_{ads} (M^{-1})$	$-\Delta G_{ads}^{\circ} (KJ.mol^{-1})$	R^2
P1	1.45E+05	40.70	0.9999

In the present study, the values of ΔG_{ads}° for P1 is $-40.70 \text{ kJ mol}^{-1}$. In the literature, if the absolute values of ΔG_{ads}° are less than 20 kJ mol^{-1} consistent with the electrostatic interaction between the charged metal and charged molecules (physisorption), but if those more than 40 kJ mol^{-1} involve sharing or transfer of electrons from the inhibitor compound to the metal surface to form a co-ordinate type of bond (chemisorption) [25, 27]. These values of ΔG_{ads}° suggest chemisorption mechanisms between mild steel and the studied inhibitor molecules [28].

3.3. Polarization curves

Potentiodynamic polarization curves have been recorded for carbon steel in 1 M HCl solution in different concentrations of P1 at 308 K (Figure 4). Electrochemical parameters extracted from polarization curves including corrosion potential (E_{corr}), corrosion current density (I_{corr}), cathodic Tafel slopes (β_c) and anodic Tafel slopes (β_a) have been measured by Tafel extrapolation and presented in Table 2.

It can be seen from Figure 4 that the existence of inhibitor molecule in the corrosive medium increases anodic and cathodic over potentials, and decreases corrosion current (I_{corr}). These changes increase with increasing inhibitor concentration. This behavior supports the adsorption of inhibitor onto metal surface and causes a barrier effect for mass and charge transfer for anodic and cathodic reactions. The cathodic potential diagrams (Figure 4), which give rise to parallel lines, show that increasing concentrations of P1 do not change the cathodic reduction reaction mechanism of hydrogen. Thus, the mechanisms of hydrogen evolution and the reduction of H^+ ions at the mild steel surface occur mainly through a charge transfer mechanism. The cathodic Tafel slope (β_c) show slight changes with the addition of P1, which suggests that the inhibiting action occurred by simple blocking of the available cathodic sites on the metal surface, which lead to a decrease in the exposed area necessary for hydrogen evolution. There is no definite trend observed in the E_{corr} values in the presence of P1. In literature [29-30], it has been reported that (i) if the displacement in E_{corr} is $> 85 \text{ mV}$ with respect to E_{corr} , the inhibitor can be seen as a cathodic or anodic type and (ii) if displacement in E_{corr} is < 85 , the inhibitor can be seen as mixed type. In the present study, shift in E_{corr} values is in the range of 4 mV , suggesting that P1 acted as a mixed type of inhibitor [31-32].

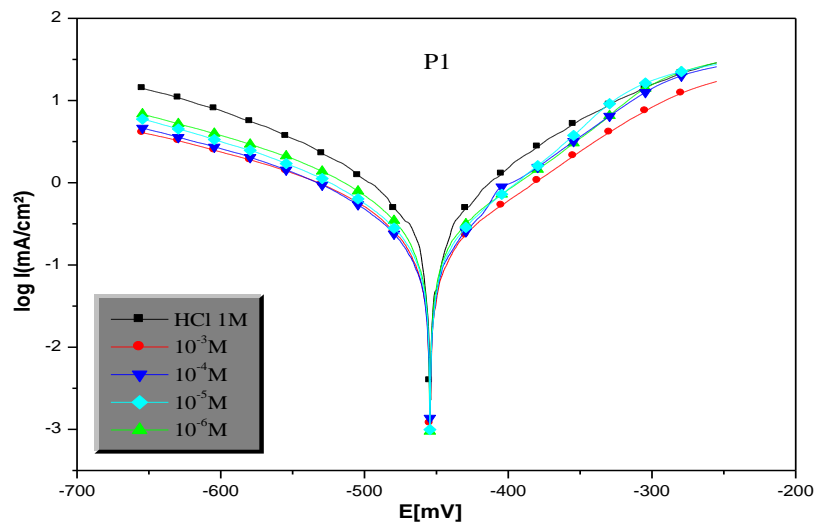


Figure 4: Potentiodynamic polarization curves for mild steel at 308 K in 1M HCl solution in the absence and the presence of P1 at various concentrations.

Table 2: kinetic parameters calculated from P1 measurements after 30min of immersion in 1M HCl solution with and without inhibitor concentrations at 308K.

Inhibitor	Concentration (M)	E_{corr} (mV/SCE)	I_{corr} ($\mu A cm^{-2}$)	β_a (V dec ⁻¹)	$-\beta_c$ (V dec ⁻¹)	E_p (%)
1M HCl	--	-459	1381	174	299	--
P1	10^{-6}	-463	454	162	302	67
	10^{-5}	-457	346	151	278	75
	10^{-4}	-461	239	181	285	83
	10^{-3}	-459	121	147	307	91

3.4. Electrochemical impedance spectroscopy (EIS) measurements

The corrosion behaviour of mild steel in 1 M HCl solution in the absence and presence of different concentrations of P1 was further investigated using EIS measurements. The Nyquist and Bode plots for mild steel in 1 M HCl without and with various concentrations of the studied inhibitor are shown in Figures 5 and 6. The Nyquist plots show depressed semicircles due to non-ideal behaviour of the electrochemical interface of mild steel in the aggressive electrolytes [33]. The diameter of Nyquist plots increases with increasing the concentration of inhibitor [34]. This suggests that the inhibitors form protective film on the steel surface thereby increasing the impedance of mild steel interface to electrochemical corrosion.

The Bode phase angle plots show two maxima corresponding to two time-constants, suggesting that the corrosion process is not just a single charge transfer reaction but might involve more complex phenomena.

The Bode impedance modulus plots exhibit linear portions at intermediate frequencies. The linearity of $\log|Z|$ vs $\log f$ plots at intermediate frequencies is more pronounced in the presence of the inhibitor, indicating higher slopes pseudo-capacitive behaviour of the electrode interface [35]. The EIS spectra were fitted into the equivalent circuit shown in Figures 7 and 8, and the electrochemical parameters obtained from the fitting and simulation analysis are listed in Table 3.

The R_{ct} value may be interpreted as the resistance of the inhibitor to the charge transfer upon oxidation of the metal. It is apparent from the results in Table 3 that the addition of inhibitor increases the R_{ct} values due to the formation of protective film of inhibitor molecules on the mild steel surface thereby reducing the transfer rate of charged species across the interface. The C_{dl} values in the presence of the inhibitor are generally lower than that of the blank acid system. This suggests a decrease in local dielectric constant or an increase in the thickness of capacitive layer, which is attributed to the adsorption of inhibitor molecules on the mild steel surface [35]. The %E increases with increasing concentration of the inhibitor but the trend of inhibitive performances obtained from the EIS data cannot be generalized.

Table 3: Electrochemical parameters for mild steel in 1 M HCl without and with different concentrations of (P1) at 308K.

Parameters	Concentration (M)				
	1M HCl	10 ⁻⁶	10 ⁻⁵	10 ⁻⁴	10 ⁻³
Real Center	9.25	32.51	43.755	48.498	62.77
Imag. Center	1.62	12.334	34.167	14.367	27.14
Diameter	15.13	65.797	111.23	96.674	134.36
Deviation	0.15	1.0861	3.7663	1.0385	2.75
Low Intercept R _s (Ω.cm ²)	1.86	2.0116	0.12582	2.3454	1.31
High Intercept R _t (Ω.cm ²)	16.64	63.009	87.635	94.65	124.22
Depression Angle	12.42	22.019	37.906	17.291	23.83
ω _{max} (rad s ⁻¹)	929.60	262.04	164.92	167.33	134.54
Estimated R _t (Ω.cm ²)	14.78	60.997	87.761	92.305	122.91
Estimated C _{dl} (F.cm ⁻²)	7.11 E-5	6.7999E-5	6.4515E-5	6.1818E-5	5.53 E-5
E (%)	--	76	83	84	88

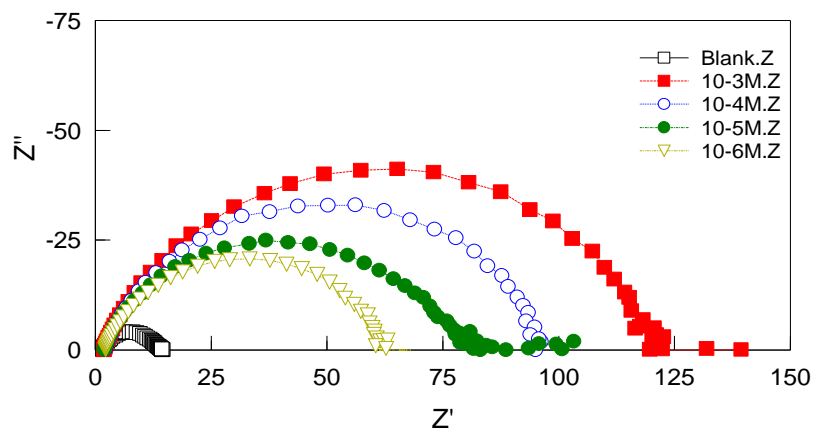


Figure 5: Nyquist diagram for mild steel in 1 M HCl in the absence and presence of P1.

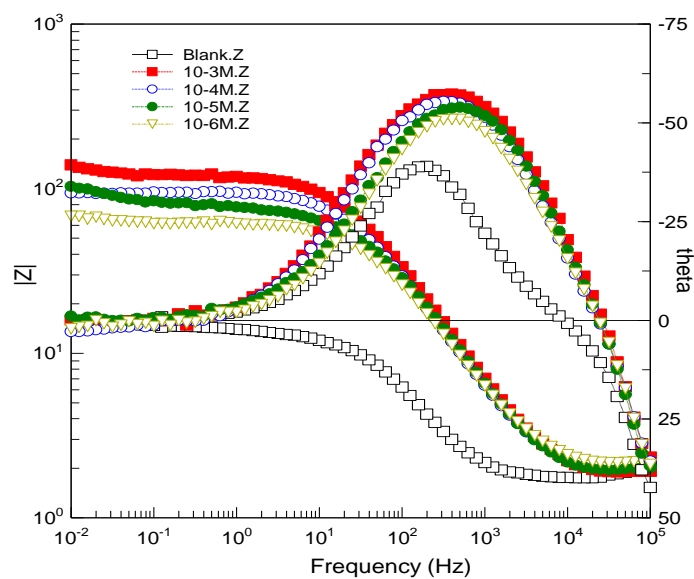


Figure 6: Bode and phase plots of mild steel in 1.0 M HCl and in the presence different concentrations of P1 at 308 K.

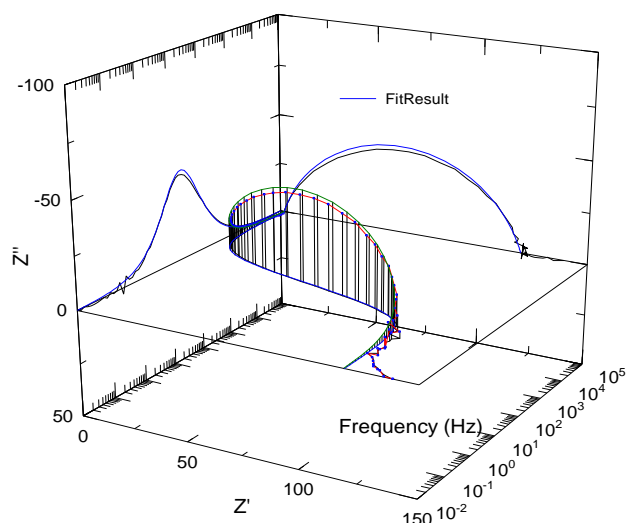


Figure 7: EIS Nyquist and Bode diagrams 3D for mild steel/1 M HCl + 10^{-3} M of P1 interface: (---) experimental; (---) fitted data.

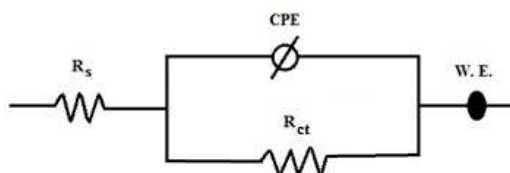


Figure 8: Equivalent circuit model used to fit the impedance spectra

3.4. Quantum chemical calculations

The FMOs (HOMO and LUMO) are very important for describing chemical reactivity. The HOMO containing electrons, represents the ability (E_{HOMO}) to donate an electron, whereas, LUMO haven't not electrons, as an electron acceptor represents the ability (E_{LUMO}) to obtain an electron. The energy gap between HOMO and LUMO determines the kinetic stability, chemical reactivity, optical polarizability and chemical hardness–softness of a compound [36]. Firstly, in this study, we calculated the HOMO and LUMO orbital energies by using B3LYP method with 6-31G which is implemented in Gaussian 09 packadge [37-38]. All other calculations were performed using the results with some assumptions. The higher values of E_{HOMO} indicate an increase for the electron donor and this means a better inhibitory activity with increasing adsorption of the inhibitor on a metal surface, where as E_{LUMO} indicates the ability to accept electron of the molecule. The adsorption ability of the inhibitor to the metal surface increases with increasing of E_{HOMO} and decreasing of E_{LUMO} . The HOMO and LUMO orbital energies of the P1 inhibitors were performed and were shown in Table 4 and Figure 9. High ionization energy (> 6 eV) indicates high stability of P1 inhibitor [39], the number of electrons transferred (ΔN), dipole moment, Ionisation potential, electron affinity, electronegativity, hardness, Softness and total energy were also calculated and tabulated in Table 4.

Table 4: Quantum chemical parameters for P1 obtained in gas and aqueous phase with the DFT at the B3LYP/6-31G level.

	μ (Debye)	HOMO	LUMO	Gap	I	A	χ	η	ω	ΔN
A	6.41	-5.77	-1.08	4.68	5.77	1.08	3.42	2.34	2.50	0.78
G	9.25	-6.18	-2.40	3.77	6.18	2.40	4.29	1.88	4.88	0.71

The value of ΔN (number of electrons transferred) show that the inhibition efficiency resulting from electron donation agrees with Lukovit's study [40]. If $\Delta N < 3.6$, the inhibition efficiency increases by increasing electron donation ability of these inhibitors to donate electrons to the metal surface [41].

Pertinent valence and dihedral angles, in degree, of the studied inhibitor calculated at B3LYP/6-31G(d,p) in gas and aqueous phases are given in the table 5.

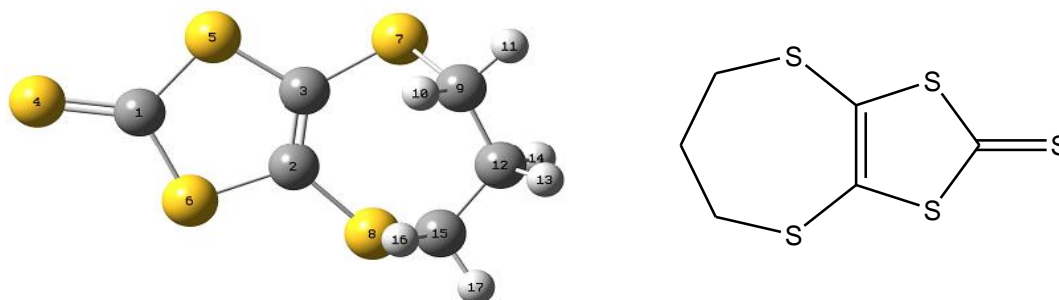


Figure 9: optimized structure of inhibitor P1

After the analysis of the theoretical results obtained, we can say that the molecule **P1** have a non-planar structure. In fact, the 1,4-dithiepane rings is it consists of two planes circa perpendicular to each other.

Table 5. Pertinent valence and dihedral angles, in degree, of the studied inhibitors calculated at B3LYP/6-31G(d,p) in gas, G and aqueous, A phases

Angle	phase	value
[S ₄ C ₁ S ₅]	G	124.2
	A	124.0
[C ₃ S ₇ C ₉]	G	102.7
	A	103.0
[S ₄ C ₁ S ₅ C ₃]	G	-177.6
	A	177.5
[C ₃ S ₇ C ₉ C ₁₂]	G	78.1
	A	-77.7

Table 6 displays the values of the Fukui functions (f^+ and f^-) of the studied inhibitors. The calculated values of the f_k^+ for inhibitors are mostly localized on the sulfur atoms, namely S₄, S₅, S₆ and C₁, indicating that the dithiolo[4,5-b][1,4]dithiepine ring will probably be the favorite site for nucleophilic attacks.

Table 6: Condensed Fukui indices calculated with Hirshfeld charges of heavy atoms in P1 inhibitor. The electron density was calculated at the DFT B3LYP/6-31G (d,p) level of theory *in gas (G) and aqueous phases*.

Gas			Aquous		
Atom	f^-	f^+	Atom	f^-	f^+
C1	0,1002	-0,0435	C1	0,1240	-0,0440
C2	0,0250	0,0138	C2	0,0041	0,0451
C3	-0,0054	0,0441	C3	0,0041	0,0451
S4	0,4618	0,2290	S4	0,3842	0,3367
S5	0,1160	0,2037	S5	0,1882	0,1595
S6	0,1180	0,2019	S6	0,1882	0,1595
S7	0,0639	0,1033	S7	0,0363	0,1129
S8	0,0634	0,1038	S8	0,0363	0,1129
C9	-0,0207	0,0183	C9	-0,0003	-0,0039
H10	0,0016	0,0172	H10	0,0055	0,0138
H11	0,0265	0,0262	H11	0,0078	0,0167
C12	0,0172	-0,0349	C12	-0,0023	-0,0044
H13	0,0127	0,0410	H13	0,0066	0,0135
H14	0,0011	0,0260	H14	0,0044	0,0099
C15	-0,0093	0,0068	C15	-0,0003	-0,0039
H16	0,0001	0,0187	H16	0,0055	0,0138
H17	0,0281	0,0246	H17	0,0078	0,0167

The strong inhibitory efficacy of this compound is due to its high sulfur.

4. Conclusion

The following main conclusions are drawn from the present study:

- The corrosion rate of mild steel increases with increasing HCl acid concentration (10^{-6} - 10^{-3})M showing first order corrosion reaction without changing the reaction mechanism.
- The concentration of P1 increased the rate of steel corrosion is decreased, which indicates that the inhibition of the corrosion process is produced.
- Electrochemical impedance spectroscopy results showed that the corrosion and corrosion inhibition of mild steel occurred mainly by charge transfer.
- The electrochemical results of polarization also showed that the P1 act as mixed type inhibitor, they retarded both cathodic and anodic reaction.
- The experimental results from chemical and electrochemical studies were fit Langmuir adsorption isotherm.
- Value of the standard free energy of adsorption ΔG_{ads}° , for the P1 have negative sign which indicates that the adsorption process of inhibitor molecules on mild steel surface is spontaneous.
- The quantum DFT approach may well be able to foretell molecule structures that are better for corrosion inhibition.

Reference

1. Elmsellem H., Nacer H., Halaimia F., Aouniti A., Lakehal I., Chetouani A., Al-Deyab S. S., Warad I., Touzani R., Hammouti B., *Int. J. Electrochem. Sci.* 9 (2014) 5328.
2. Bentiss F., Gassama F., Barbry D., Gengembre L., Vezin H., Lagrenée M., Traisnel M., *Appl. Surf. Sci.* 252 (2006) 2 684.
3. Ellouz M., Elmsellem H., Sebbar N. K., Steli H., Al Mamari K., Nadeem A., Ouzidan Y., Essassi E. M., Abdel-Rahaman I., Hristov P., *J. Mater. Environ. Sci.* 7(7) (2016) 2482-2497.
4. Khaled K.F., Hackerma N., *Electrochim. Acta.* 48 (2003) 2715.
5. Chakib I., Elmsellem H., Sebbar N. K., Lahmidi S., Nadeem A., Essassi E. M., Ouzidan Y., Abdel-Rahman I., Bentiss F., Hammouti B., *J. Mater. Environ. Sci.* 7 (2016) 1866-1881.
6. Hammouti B., Salghi R., Kertit S., *J. Electrochem. Soc. India.* 47 (1998) 31.
8. Hjouji M. Y., Djedid M., Elmsellem H., Kandri Rodi Y., Benalia M., Steli H., Ouzidan Y., Ouazzani Chahdi F., Essassi E. M., Hammouti B., *Der Pharma Chemica.* 8(4) (2016) 85-95.
9. Filali Baba Y., Elmsellem H., Kandri Rodi Y., Steli H., AD C., Ouzidan Y., Ouazzani Chahdi F., Sebbar N. K., Essassi E. M., and Hammouti B., *Der Pharma Chemica.* 8 (2016) 159-169.
10. Hjouji M. Y., Djedid M., Elmsellem H., Kandri Rodi Y., Ouzidan Y., Ouazzani Chahdi F., Sebbar N. K., Essassi E. M., Abdel-Rahman I., Hammouti B., *J. Mater. Environ. Sci.* 7 (2016) 1425-1435.
11. Elmsellem H., Basbas N., Chetouani A., Aouniti A., Radi S., Messali M., Hammouti B., *Portugaliae. Electrochimica Acta.* 2 (2014) 77.
12. Elmsellem H., Harit T., Aouniti A., Malek F., Riahi A., Chetouani A., Hammouti B., *Protection of Metals and Physical. Chemistry of Surfaces.* 5 (2015) 873.
13. Pearson R.G., *Inorg. Chem.* 27 (1988) 734-740.
14. Jeroundi D., Elmsellem H., Chakroune S., Hammouti B., Idouhli R., El Hadrami E. M., Ben-Tama A., Oudani M., Ouzidan Y., Kandri Rodi Y., *J. Mater. Environ. Sci.* 7 (10) (2016) 3895-3904.
15. Bentiss F., Jama C., Mernari B., El Attari H., El Kadi L., Lebrini M., Traisnel M., Lagrenée M., *Corros. Sci.* 51 (2009) 1628.
16. Zerga B., Hammouti B., Ebn Touhami M., Touir R., Taleb M., Sfaira M., Bennajeh M., ForssalInt I., *J. Electrochem. Sci.* 7(2012)471 – 483.
17. Udhayakala P., Rajendiran T. V., Gunasekaran S., *Chem. J.Biol. Phys. SCIA.* 2(3) (2012)1151-1165.
18. Roy R.K., Pal S., Hirao K., *J. Chem. Phys.* 110(1999)8236.
19. Martinez S., Metikos-Hukovic M., *J. Appl. Electrochem.* 33 (2003) 1137–1142.
20. Filali Baba Y., Elmsellem H., Kandri Rodi Y., Steli H., AD C., Ouzidan Y., Ouazzani Chahdi F., Sebbar N. K., Essassi E. M., Hammouti B., *Der Pharma.Chemica.* 8(4)(2016)159-169.
21. Lebrini M., Lagrenée M., Vezin H., Traisnel M., Bentiss F., *Corros. Sci.* 49 (2007) 2254–2269.
22. Quraishi M.A., Sharma H.K., *Chem. Phys.* 78 (2002) 18.

23. Martinez S., *Mater. Phys.* 77 (2003) 97-102.
24. Elmsellem H., Aouniti A., Youssoufi M.H., Bendaha H., Ben hadda T., Chetouani A., Warad I., Hammouti B., *Phys. Chem. News.* 70 (2013) 84.
25. Quraishi M.A., Sardar R., *Mater. Chem. Phys.* 78 (2002) 425.
26. Elmsellem H., Karrouchi K., Aouniti A., Hammouti B., Radi S., Taoufik J., Ansar M., Dahmani M., Steli H. and El Mahi B., *Der Pharma Chemica.* 7(10)(2015)237-245.
27. Sebbar N. K., Elmsellem H., Boudalia M., Iahmidi S., Belleaouchou A., Guenbour A., Essassi E. M., Steli H., Aouniti A., *J. Mater. Environ. Sci.* 6 (11) (2015)3034-3044.
28. Bentiss F., Lebrini M., Lagrenée M., *Corros. Sci.*,47 (2005) 2915.
29. Elmsellem H., Harit T., Aouniti A., Malek F., Riahi A., Chetouani A., Hammouti B., *Protection of Metals and Physical. Chemistry of Surfaces.* 51(5) (2015) 873.
30. Elmsellem H., Elyoussfi A., Sebbar N. K., Dafali A., Cherrak K., Steli H., Essassi E. M., Aouniti A. and Hammouti B., *Maghr. J. Pure & Appl. Sci.*1 (2015) 1-10.
31. El Azzouzi M., Aouniti A., Tighadouin S., Elmsellem H., Radi S., Hammouti B., El Assyry A., Bentiss F., Zarrouk A., 221 (2016) 633-643. DOI: 10.1016/j.molliq.2016.06.007
32. Elmsellem H., Aouniti A., Khoutoul M., Chetouani A., Hammouti B., Benchat N., Touzani R. and Elazzouzi M., *J. Chem. Pharm. Res.* 6 (2014) 1216.
33. Quraishi M.A., Sardar R., Jamal D., *Mater. Chem. Phys.* 71(2001) 309.
34. Ebenso E.E., Obot I.B., Murulana L.C., *Int. J. Electrochem. Sci.*, 5 (2010) 1574.
35. Elmsellem H., Youssouf M. H., Aouniti A., Ben Hadd T., Chetouani A., Hammouti B., *Russian, Journal of Applied Chemistry.* 87(6) (2014) 744.
36. Govindarajan M., Karabacak M., *Spectrochim Acta Part A Mol Biomol Spectrosc.* 85 (2012)251-60.
37. Becke A.D., *J. Chem. Phys.* 98 (1993) 1372.
38. Behpour M., Ghoreishi S.M., Soltani N., Salavati-Niasari M., Hamadani M., Gandomi A., *Corros.Sci.* 50(2008)2172.
39. Sabatini S., Kaatz G. W., Rossolini G. M., Brandim D., Fravolini A., *J. Med. Chem.* 51(2008) 4321-4330.
40. Lukovits I., Kalman E., Zucchi F., *Corrosion.* 57 (2001)3-7.
41. Sikine M., Kandri Rodi Y., Elmsellem H., Krim O., Steli H., Ouzidan Y., Kandri Rodi A., Ouazzani Chahdi F., Sebbar N. K., Essassi E. M., *J. Mater. Environ. Sci.* 7 (4) (2016) 1386-1395.

(2016) ; <http://www.jmaterenvirosci.com/>